PERGAMON

International Journal of Solids and Structures 40 (2003) 4549–4562

INTERNATIONAL JOURNAL OF SOLIDS and STRUCTURES

www.elsevier.com/locate/ijsolstr

Filler-reinforcement of elastomers viewed as a triboelastic phenomenon

V.V. Moshev *, S.E. Evlampieva [1]

Institute of Continuous Media Mechanics, Russian Academy of Science, Academic Korolev Street 1, 614013 Perm, Russia

Received 13 June 2002; received in revised form 17 February 2003

Abstract

A triboelastic approach is offered for modeling the reinforcement phenomenon in particulate elastomeric composites. The structural unit is composed of two solid substrates, modeling the surface of filler particles, and an adjoining nonlinear elastic spring, modeling a rubber molecule adsorbed by the surfaces of substrates. The strength of the adhesive bond is represented as a specified frictional resistance appearing when the string is sliding along the substrate. The tensile curve of this model gives a clearer insight into the reinforcement mechanism, which may by regarded as the frictional resistance experienced by the spring on its sliding along the substrates at lower and moderate deformations.

Keywords: Particulate elastomeric composites; Reinforcement mechanism

1. Introduction

It is well known that the solid tiny particles of a micron size or less incorporated into rubber matrices increase considerably the modulus and tensile strength of such particulate composites while retaining and sometimes even enhancing their high breaking deformations.

The mechanism of this effect discovered about 90 years ago and widely used in industry remains unclear until now. In spite of huge experience gained by chemists, physicists and mechanicians in a search for its foundation, it remains at a level of qualitative explanations not substantiated by an appropriate quantitative modeling (Alexandrov and Lazurkin, 1944; Mullins, 1987; Song, 1987; Medalia, 1987; Edwards, 1990).

This paper represents an attempt to develop a mathematical model based on the concepts evolved by Alexandrov and Lazurkin (1944), Dannenberg (1966), Rigbi (1980), Soos (1984), Medalia (1987) and Edwards (1990), who suggested that it is the surface mobility and dragged slippage of elastomeric molecules

* Corresponding author.
E-mail address: moshev@icmm.ru (V.V. Moshev).
[1] Present address: Raboche-Krestyanskaya Street, 30-93, 614007 Perm, Russia.

0020-7683/03/$ - see front matter © 2003 Elsevier Ltd. All rights reserved.
doi:10.1016/S0020-7683(03)00145-8

adsorbed on the surface of submicron filler particles that play the leading part in the reinforcement phenomenon.

2. Experimental evidence of the reinforcement effect with attendant whys and wherefores

The quantitative evaluation of reinforcement is usually represented as the ratio of the strength of a filler-reinforced elastomer to that of a gum vulcanizate, other factors being the same, or as the ratio of the modulus of the filler-reinforced elastomer to that of the gum vulcanizate at some specified elongation (usually about 300%).

The experience gained is presented in a number of thorough reviews (Mullins, 1969; Kraus, 1978; Boonstra, 1979; Rigbi, 1980; Voet, 1980; Medalia, 1987; Edwards, 1990). They allow us to summarize conditions, which cause the reinforcement effect and may be regarded as the experimental evidence for the creation of an appropriate mathematical simulation.

The augmentation of the area of contact between the rubber binder and the filler particles appears to be of key factor importance in providing the pronounced reinforcement effect. The value of the interface contact area is determined both by the size of filler particles and their volume fraction (Mullins, 1969; Kraus, 1978; Boonstra, 1979; Edwards, 1990; Yuan and Mark, 1999) with the chemical nature of particles being of minor importance (Voet, 1980; Edwards, 1990). The size of filler particles is of primary concern. Since the interface contact area increases as the reciprocal of the particle diameter, the use of micron and submicron-sized filler furnishes the largest interface areas with ultimate reinforcement effects (Boonstra, 1979; Kraus, 1978; Medalia, 1987). In addition, the interface area grows with the filler volume fraction. The reinforcement caused by this factor reaches maximum at about 0.2–0.3 filler volume fraction (Kraus, 1978; Boonstra, 1979; Edwards, 1990).

The reinforcement is most pronounced in elastomers based on flexible hydrocarbon molecules capable of large elongation ratios upto 15 with a sharp upward nonlinear increase in stiffness before the breakdown due to the limited chain extensibility (Edwards, 1990; Yuan et al., 1996; Bokobza, 2001).

Next important aspect of elastomer reinforcement is a degree of bonding between the filler particles and the rubber chains on the interface. Generally, this magnitude varies widely from a very weak physical interaction, as in the case of the graphitized carbon black (Kraus, 1978), to nearly complete chemical immobilizing of the rubber at the filler surface. Experience demonstrates a profound effect of the filler-rubber interaction on the reinforcement effect. Excessive chemical bonds promote the reduction of both breaking stresses and strains (Edwards and Fischer, 1973). Weak covalent bonds prevent obtaining the desirable modulus magnitudes.

A number of scientists, who examined the reinforcement phenomenon (Alexandrov and Lazurkin, 1944; Dannenberg, 1966; Rigbi, 1980; Soos, 1984; Medalia, 1987; Edwards, 1990; Kilian et al., 1994; Leblanc, 1995; Kaliske and Rothert, 1998), attributed it to the surface mobility and dragged slippage of adsorbed segments of elastomer chains over the surface of filler particles, assuming that this process prevented molecules from premature breaking and thus increased the resistance of material to extension. They believed that the dragged slippage played a decisive role in the phenomenon under consideration.

These concepts have been well supported by experience. It is known that hysteretic losses in cycling filled rubbers are essentially high and their magnitude grows with sample elongation. Grosch et al. (1966) have established an unexpected general regularity lying in the fact that the more the energy accumulated in the break-down extensions, the more the attendant hysteretic loss. If one regards this loss as a manifestation of the microdamage accumulation, then it remains unclear why the failure energy should increase with the growth of the accumulated damage. However, if the hysteretic loss is looked upon only as a result of a dragged slippage of adsorbed rubber molecules over the surface of filler particles, then the hysteretic effect

can be conceived of as a measure of the internal structural rearrangement that has nothing to do with damage emergence and accumulation.

Tensile cycling of filled rubbers at constant amplitudes commonly leads the tested samples to some steady degree of softening with negligible residual hysteretic losses (Soos, 1984; Kovrov and Moshev, 1984; Eisele and Müller, 1990). The tested sample behaves as if it again approaches the elastic state, which is very distinct from the initial one (the convex shape of tensile primary curves transforms into the concave one). At first glance, it seems that cycling at constant amplitude provokes an establishment of some constant degree of damage responding to the imposed strain amplitude. Increasing amplitude enhances softening with subsequent stabilization of a new elastic behavior.

Subsequent experiments, however, disclosed that this interpretation is untrue. Soos (1984) experimentally found that the hysteretic losses, he observed in cycling tests of the carbon black filled rubber, can in no way be regarded as an evidence of irreversible damaging of tested material. After heating the cycled specimens at 120 °C for several hours, he restored the initial properties of the tested samples. Restoring the initial mechanical behavior of specimens implied that the basic properties of their constitutive elements (rubber and filler) were not changed by cycling. Then some questions arise as to why cycling provokes specimen softening; why this softening becomes stable after several cycles; why heating restores the initial properties of specimens.

The hypothesis for the interface dragged slippage during deformation of particulate composites seems to be well suited for answering these questions. Slippage, provoked by specimen extension and realized through overcoming adhesive bonding, changes the internal structure of the composite system. Newly formed adhesive linkages preserve this state, since the weak enthropic retractive elasticity is unable to revert the system to its initial state. Heating slackens the adhesive bonds and enhances the enthropic retractive force, which leads to restoring the original state of the specimen.

Since adhesive bonds resist rubber slipping both under extension and retraction, the cycling of specimens provides hysteretic loops. Clearly, they have nothing to do with damage accumulation, because these hysteretic losses characterize only the degree of reversible structural rearrangement taking place at the filler-rubber interface. Hence, a higher hysteretic loss means simply higher degree of the internal structural rearrangement. From this point of view, the experimental results obtained by Grosch et al. (1966) might be interpreted as follows: the more the filled rubber is capable of reversible structural rearrangement during deformation, the higher the work done at break. Remembering that the slippage of rubber molecules over the surface of the filler particle is the cause of structural rearrangements, we may conclude that it is directly related to the strength of rubbery particulate composites.

The main topic of our study has been directed to a creation of a primary structural model capable to explain in *a quantitative* manner the reinforcement effect observed in experiments, what, to our knowledge, has not yet been done. Since the bulk of available experimental data on the reinforcement phenomenon has been obtained in simple tension, this kind of extensive experimentation was chosen first as the base to start with.

3. Modeling the reinforcement mechanism in terms of triboelastic approach

At present, a quantitative micromechanical description of the rubber-filler interaction based on the rigorous molecular dynamics examination seems to be unlikely due to the complexities in the representation of the irregular shape of filler particles, arrangement of the adsorbed macromolecules over the contact surface and their movements under the action of the applied external forces. With this in mind, we have made an attempt to create a rougher approach still retaining dominant factors responsible for the reinforcement effect, i.e., the mechanical properties of rubber molecules with their limited chain extensibility

and the ability of adsorbed molecules for dragged sliding along the interface under the applied pulling action.

3.1. Simulation of rubber molecules mechanical behavior

Many authors (Zhang and Mark, 1982; Boue and Vilgis, 1986; Mohsin and Treloar, 1987; Diamant et al., 1988; Yuan et al., 1996) claim that the capacity of rubber molecules to increase essentially the elastic stiffness in extension before breaking plays an important role in the reinforcement phenomenon. In this connection, it seemed appropriate to simulate, as close as possible, the resistance of macromolecular chains to extension by that of the nonlinear elastic springs. According to Treloar (1958), the elongation, λ, of flexible rubber molecules under extension can be expressed as

$$\lambda = \lambda_m(\mathrm{Cth}f - 1/f), \tag{1}$$

where f is some dimensionless measure of the tensile force, λ_m is an ultimate elongation ratio of the molecule, which depends on the contour length L_0 of the molecule expressed as a number, N, of freely joint segmental units composing the given molecule.

$$\lambda_m = \sqrt{N}. \tag{2}$$

With this in mind, for selecting the properties of modeling elastic springs, we have adopted the expression rather close to that emerging from the molecular concepts

$$\lambda = \lambda_m(\mathrm{Cth}f - 1/f) + 1.0, \tag{3}$$

where λ is the elongation ratio of the spring under the tensile force f with λ_m being the breaking value of λ. This expression reflects the basic feature of the molecular behavior: a constant initial modulus with the consequent steep nonlinear upturn until breakdown.

Again, as in case (2) for freely joint molecular segments, it has been adopted that breaking elongation ratio λ_m for the modeling spring depends on its length L_0 as follows

$$\lambda_m = \sqrt{L_0}. \tag{4}$$

Here, as in Eq. (2), the length L_0, as well as other length measures, should be regarded as expressed through a dimensionless number of some segmental units composing its length.

Combining (3) and (4) yields

$$\lambda = \sqrt{L_0}(\mathrm{Cth}f - 1/f) + 1.0, \tag{5}$$

where L_0 is the segmental length of the spring, and f is the tensile force in dimensionless form. This expression is taken for modeling the tensile behavior of rubbery molecules with the nonlinear elastic springs.

Returning to the basic expression (1), let us establish the breaking elongation for modeling springs. Obviously, an infinite force required by (1) for perfect stretching of rubber molecules is highly improbable. Apparently, rubber molecules should break at lesser stretches. As far as we know, reliable data concerning breaking elongations of single rubber molecules are missing. However, the approximate theoretical calculations made by He (1986) allow one to make rough estimates of actual breaking elongations, λ_b, of rubber chains. If the thermal fluctuations and scatter in individual chain loadings are accounted for, the carbon-carbon bonds most likely break down at elongation close to 0.95 of the λ_m value. Then the breaking force of the molecule, f_b, related to this condition, immediately follows from (1). It should be taken equal to 20.0. This criterion has been adopted as the breaking force for springs modeling the behavior of molecules.

We shall define the deformation of the spring, ε, as

$$\varepsilon = \Delta L/L_0, \tag{6}$$

where ΔL is the increase in the length of the spring under the action of the force f.

Hence

$$\Delta L = L_0\sqrt{L_0}(\mathrm{Cth}f - 1/f). \tag{7}$$

As follows from (5), the tensile behavior of elastic springs, modeling rubber molecules, is of a rather specific kind. By contrast to usual elastic springs, their stiffness becomes a function of their length, their initial modulus is a constant equal to 3, and their breaking stress is also a constant equal to 20. Fig. 1 demonstrates tensile curves for various lengths of modeling springs. The initial nearly linear increase of the force gives way to strongly pronounced nonlinearity of tensile curves with steep upturns ending in identical breaking forces. A marked dependence of breaking deformations on the length of springs is a key feature of the rubber molecule behavior simulation.

3.2. Filler-rubber adsorption bond modeling

To our knowledge, there are no data on this point that are workable in simulation adsorption bond. Nonetheless, a close similitude of adhesive failure under shear and interface sliding friction can be easily traced. That is the reason why, in the scheme outlined below, the failure of the adsorption bond is simulated by some specific friction force. This approach takes the bond energy as some constant specific property. Hence, it postulates the sliding friction per unit interface length, T, to be some constant magnitude. Similar assumptions on adsorption phenomenon are encountered in papers of some physicists (Heinrich and Vilgis, 1995). No sliding occurs at interface shear stresses that are less than T. Hence, the force, f, needed to provide sliding along the length of the solid substrate, u, is easily obtained as

$$f = Tu. \tag{8}$$

In order to avoid using dimensional magnitudes, it is adopted that force unit for T is the same dimensionless magnitude as that for f in expression (5).

3.3. The primary triboelastic structural element

The above constitutive elements enable assembling a unitary construction of a primary triboelastic structural element, designed for modeling the reinforcement phenomenon. Its geometry, shown in Fig. 2, is composed in such a way as to elucidate the triboelastic nature of the reinforcement in a most distinct manner.

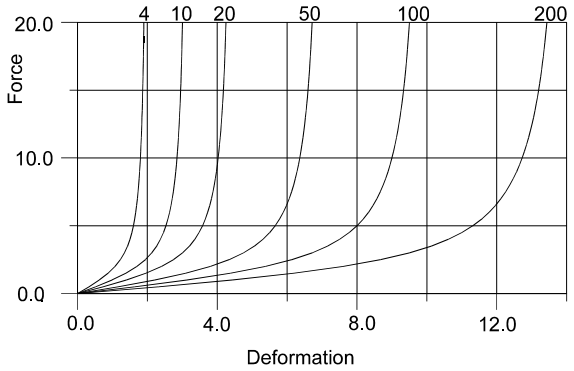

Fig. 1. Tensile curves for various lengths of modeling strings. Number near the curves indicate segmental lengths of the springs.

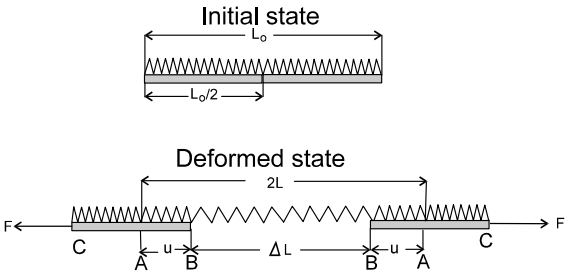

Fig. 2. Primary triboelastic structural element.

A spring of length L_0 is located along two substrates of equal length ($L_0/2$), representing neighboring filler particles. The left and right ends of the spring are clamped to the left and right external ends of substrates. Both substrates are supposed to have identical interface friction, T. Initially, the system is assumed to be free of internal stresses.

The tensile force F is applied to the model for demonstrating and analyzing the reinforcement phenomenon. The bridge ΔL of a stressed spring appears once the extension has started (Fig. 2). It is formed by the portions of the extending spring, which have slipped from the substrates into a widening gap between them. Clearly, the bridge between the substrates experiences the same tensile force f as that applied to the model.

The extension passes through two stages. At the outset, the rising resistance of the model stems only from the interface friction between the spring and the substrates due to the increasing sliding length u. The stress in the spring originates at points A and grows linearly (according to (8)) till points B, where it reaches the maximum value uT transmitted to the frictionless bridging zone ΔL of the spring. Portions of the spring lying outside points A remain free of stresses. The state, where the response of the model to extension is controlled solely by the interface friction, goes on until the interface sliding reaches points C having covered completely the substrate lengths $u_m = L_0/2$.

Then the proper elastic stiffness of the spring also becomes engaged into the elastic resistance, in parallel with the frictional one. This system breaks down in its most stressed locality, i.e., somewhere in the gap between the substrates, when the tensile force applied to the model reaches the maximum postulated value 20.0.

The calculation of the tensile curve for the model in Fig. 2 is carried out as follows. For the sake of convenience, the force of extension, F, is introduced as a leading parameter. Considering the symmetry of the model in Fig. 2, for simplicity, a half-sized part of the model will be further mathematically treated.

According to (8), applying F immediately actuates the sliding of the spring along the portion u of the substrate

$$u = F/T, \tag{9}$$

adjoining the gap between the substrates. So, the initial (reduced) length of the spring, L, involved in sliding equalizes u.

Under the action of the force, F, the initial length of the spring L increases and partly goes out of the frictional contact with the substrate, forming the bridge between substrates. The reduced length L now may be regarded as a sum of a certain length S, retained by friction on the substrate along the section u, and a length R gone out from the friction zone,

$$L = S + R. \tag{10}$$

Taking into account that the force in the spring varies along the frictional contact u increasing linearly from zero at points A to F at points B, the value of S can be found by the appropriate integration procedure. Each element du on the substrate is in one-to-one correspondence with the spring element dS, stretched along du by the local effort f, i.e.

$$dS = du/\lambda, \tag{11}$$

where λ is the elongation ratio at the point under consideration. λ depends both on the current value f and the reduced length of the spring involved in movement, which is equal to $2L$ according to the adopted scheme of the model shown in Fig. 2. Hence

$$dS = du/\left(\sqrt{2L}(\mathrm{Cth}f - 1/f) + 1.0\right). \tag{12}$$

Summing dS over u one determines the frictionally restrained length of the spring S corresponding to the zone u for one substrate

$$S = \int_0^F \frac{(df/T)}{\sqrt{2L}(\mathrm{Cth}f - 1/f) + 1.0}. \tag{13}$$

Now the frictionless length of the spring, R, slipped off from each substrate is found as

$$R = L - S. \tag{14}$$

Thus, the reduced length of the spring joining substrates within the gap should be taken equal to $2R$.

According to (7), the stretch of the bridged portion of the spring ΔL is equal to

$$\Delta L = (2R)\left(\sqrt{2L}(\mathrm{Cth}F - 1/F) + 1\right). \tag{15}$$

The deformation of the model, ε, is defined as

$$\varepsilon = \Delta L/(2L). \tag{16}$$

Following the above scheme, the extension comes to an end when u reaches points C (Fig. 2). It is seen that the second stage of deformation starts, when the reduced length of the spring remains constant, equal to Lo with the 'frictional' resistance stabilized at level $F_1 = T(Lo/2)$. Now the sought-for value of S is calculated as

$$S = \int_{F_1}^{F+F_1} \frac{(df/T)}{\sqrt{L_0}(\mathrm{Cth}f - 1/f) + 1.0}.$$

Here, the upper limit represents the tensile force applied to the model.

Subsequent treatment is similar to the above examined with

$$\begin{aligned} R &= L_0/2 - S, \\ \Delta L &= (2R)\left(\sqrt{L_0}(\mathrm{Cth}(F + F_1) - 1/(F + F_1)) + 1\right). \end{aligned} \tag{17}$$

The cell breaks down when the tensile force applied to the model $(F + F_1)$ reaches the adopted breaking value 20.0.

A like computational scheme is used in solving tasks with other loading schedules. It consists in imposing the force, F, and calculating the reduced length of the moving part of the spring L, the reduced dragged length, S, the reduced free length, R, and, finally the increase in the length of the model, ΔL. For more details, see Appendix A, where an example of hysteresis cycles calculation is presented.

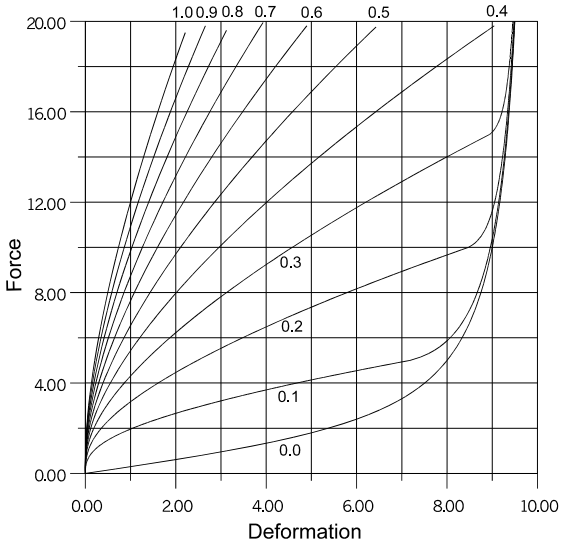

Fig. 3. Tensile curves of the structural elements at various interface friction.

3.4. Basic features of the primary triboelastic structural element

Fig. 3 demonstrates a set of tensile curves obtained for $L_0 = 100$ (Fig. 2) in a wide range of friction values, T, indicated at the curves. The lower concave down curve represents the behavior of the non-dragged freely moving spring characterized by a very low initial modulus upto about 400%. Such a shape makes a sharp contrast to other convex upward curves caused by the triboelastic manifestation. This distinction is of fundamental importance.

It becomes evident that the appearance of the friction between the spring and the substrate causes a considerable increase in the resistance of the model just in the range of deformations (upto 5), where a proper resistance of the string is remains still low.

It develops that a several time reinforcement is reached even at moderate friction values of the order of 0.2–0.4. For instance, at strains about 300%, the reinforcement factor about 9 for the specific friction equal to 0.3 is gained.

Next point worthy of attention is that, within the range of moderate friction forces, upto 0.4, the breaking strains remain identical with those of the free string. At higher specific frictions a steep drop of breaking strains takes place. The role of friction provoking a raise of the resistance at the initial stages of extension dies out as the force approaches the breaking value of 20.0.

The specific combination of the upturn nonlinear elasticity of the string, modeling the behavior of rubber molecules and the convex frictional resistivity, is, perhaps, the main cause of rubber reinforcement. Qualitatively, these results are consistent with the experimental observations that just moderate filler-rubber couplings are favorable for getting resilient rubbers with reasonably high reinforcement (Edwards and Fischer, 1973; Rivin and True, 1973).

4. Evaluation of the predictive capabilities of the triboelastic modeling and discussion

The frictional sliding of the elastic spring along the substrates in the framework of the model in Fig. 2 might, obviously, provokes the hysteresis manifestation in cycling tests. The hysteresis stems from the

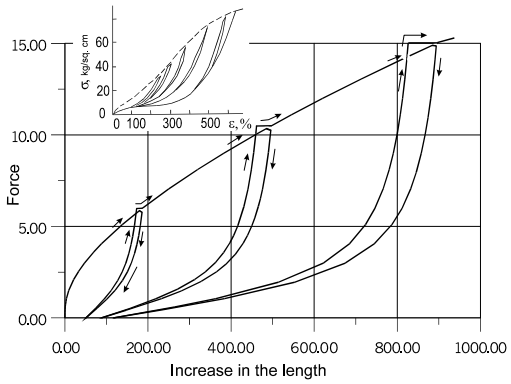

Fig. 4. Tension-retraction cycles with the increasing amplitudes indicated near the loops for $T = 0.3$.

inability of the extended string elements, positioned along the filler-rubber interface during extension stage, to return completely to their initial localizations during retraction, since the elastic retractive force of the spring meets the opposing frictional resistance.

Fig. 4 demonstrates the calculated tension-retraction cycles with the increasing amplitudes for the basic model in Fig. 2. Experimental cycles are depicted in the insert (Kovrov and Moshev, 1984). Both the measurement and computation agree on the main feature of such testing, i.e., the one-time tensile curve restoring contrary to softening induced by intermediate cyclings. The deviation between them, wherein cycles are coupled, comes from the deficiency of the model that neglects extenuating action of relaxation phenomenon. In no way it can influence restoring mechanism.

It is obvious that the hysteresis under investigation can not be considered as a kind of structural damaging, since the system can be reverted to the initial state by eliminating the interface friction. In practice, this can be realized by heating the cycled specimens, as was demonstrated by Soos (1984).

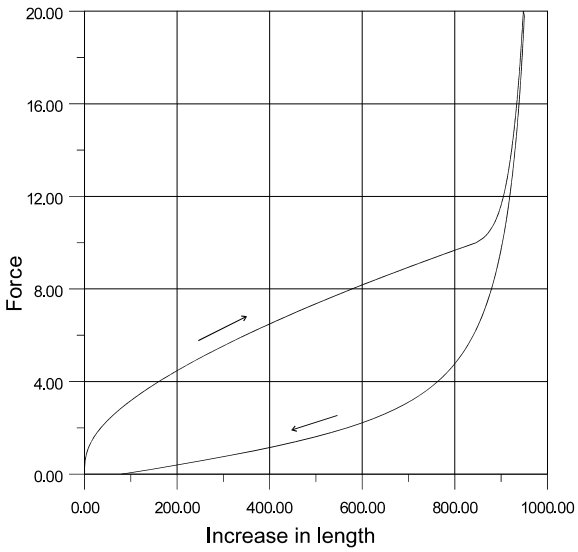

Fig. 5. Typical shape of hysteresis loop in a just before rupture state.

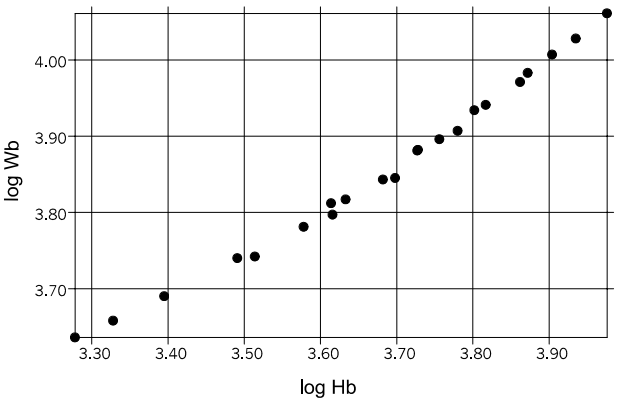

Fig. 6. W_b vs. H_b calculated from numerical experiments.

The scheme of the model adopted allows one to calculate the work done at break, W_b, and the hysteretic loss, H_b, corresponding to this state. One typical shape of such hysteretic loop is shown in Fig. 5. Now we can compare the theoretical W_b vs. H_b correlation so obtained with the well known experimental data established by Grosch et al. (1966). Fig. 6 presents log W_b vs. H_b relation computed for a set of input data with specific friction varying between 0.1 and 1.0 and the lengths of the initial gap between the substrates varying from zero to 0.8 of the length of the spring taken to be 100. The points fall closely to a single curve that after statistical treatment provides the equation

$$W_b = 37.8H_b^{0.62}.$$

Qualitatively, this equation, agrees well with the experimental relationship established by Grosch et al. (1966)

$$W_b = 4.1H_b^{0.67}.$$

This suggests that the triboelastic participation explains, to some extent, the nature of the experimentally established relationship between W_b and H_b that until now has remained, as far as we know, rather unclear.

Seemingly, the examined triboelastic model must be viewed only as a primary structural element of rubbers filled with submicron-sized particles. It reflects some features of these materials. However, it can not predict other important macroscopic properties (such as the strength and ultimate elongation of composites) that are beyond the explanatory capabilities of a single structural unit. The macroscopic properties are formed on higher dimensional levels characterized by a considerable structural nonhomogeneity. Thus, the subsequent development of multilevel modeling seems to be imperative.

Another point worthy of attention is the contribution of dangling chains and available free chains to the reinforcement effect. Obviously, these ones, adsorbed on the neighboring particles, should be engaged in the elastic resistance so long as the spacing between the particles remains less than the proper length of such chains. The approach examined in this paper seems to be well suited for quantitative evaluation of the role of these so-called "defective" network elements in the reinforcement of particulate composites.

Considering the reinforcement phenomenon as a whole, it is commonly believed that the reinforcement is a way of *rubber network* strengthening. However, on the basis of this postulate, it is very difficult to explain the experiments (Kraus, 1978), where the breaking strain of filled rubbers, along with the considerable increase in strength, turns out to be three–four times greater than that of the unfilled rubber network. It may be safely suggested that the role of the rubber network structure in determining ultimate characteristics of filled rubbers is unessential. Perhaps, it is the interface slip, facilitating deep rearrangements of filler

particles at high extensions that plays a dominant role in enhancing the ultimate deformations. This condition does not require the mandatory existence of the precursor rubber network structure, which was impressively demonstrated by Leblanc (1995) in his experiments with the filled non-crosslinked rubbers.

A triboelastic model considered is able to explain the relation between the chain dimensions and the size of the filler particles only on a qualitative level. Decreasing the size of filler particles, solid volume and chain dimension being kept constant, diminishes not only the space between the particles but also increases considerably the number of such shorten molecular bridges set in resistance. Remembering that stiffness of the interparticle chains increases with their shortening and the number of the counteracting units increases too one would expect significant increase in the initial modulus of the system. The quantitative estimation of the role of particle size in reinforcement demands constructing a more complicated structural model than the simplest one considered in this manuscript. We intend to investigate numerically such updated model in our next paper dedicated to the evaluation of general predictive potentialities of the triboelastic approach.

5. Conclusions

The results of this work show that the offered triboelastic model is capable of quantitative predicting the reinforcement of rubber by solid particles. The model is based on the hypothesis suggested earlier by a number of researchers, who postulated that, under the action of applied force, macromolecules adsorbed on the surface of filler particles come into the dragged sliding without breaking for some time and so promote the effect in question.

The structure of the model includes a nonlinear elastic spring simulating the properties of macromolecules, a substrate simulating the surface of filler, and the force of adhesion being represented by some effective friction resistance.

This model reflects the reinforced resistance as a result of combined action of two aforementioned mechanisms. A most distinctive feature of such a interaction is the fact that even the moderate interface friction effectively compensates a very weak initial elastic resistance of macromolecules and thus leads to a several times increase in the reinforcement of the system in the range of strains 100–400%.

Conceptually, the model consisting of one string and two substrates may be regarded as a primary structural element. Numerical experiments simulating the cycling the growing amplitudes and the calculated relation between the work at breaking and hysteresis loss are in good agreement with experimental data.

The next step in this direction seems to be a creation of mesoelements as random assembles of primary structural elements with higher predictive potentiality.

Acknowledgements

The financial support of the Russian Foundation of Fundamental Research and the Department of Science and Education of Perm Region Administration under Grant N 01-01-96492 is greatly acknowledged.

Appendix A. Scheme of calculating hysteresis cycles for up and down extension loading with increasing amplitudes

At any instant, according to Eq. (15), the increase in length ΔL of the model, shown in Fig. 2, under the load F is a stretch of the bridged portion R of the string L that is set in motion. Hence, in hysteresis cycling,

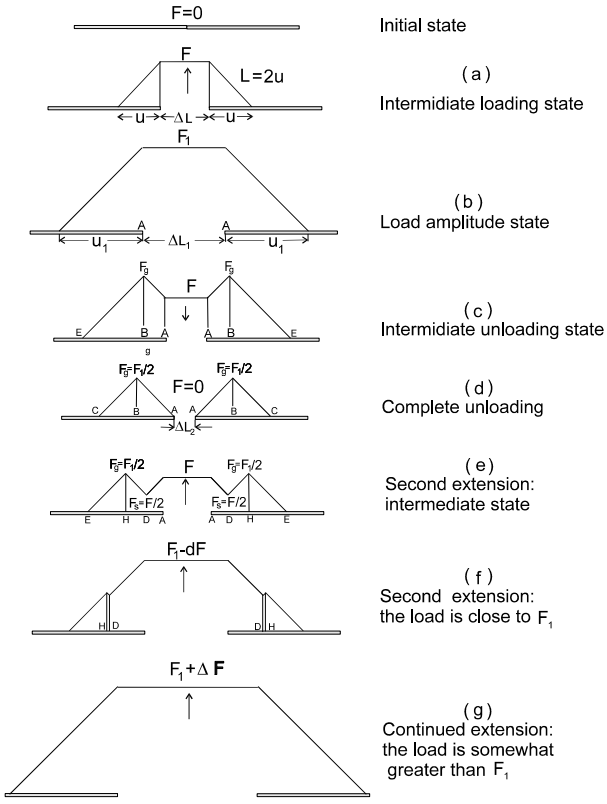

Fig. 7. Loading states in cycling.

the computation of ΔL against the imposed F variations is reduced to the establishment of L- and R-values for any specified situation.

Let the specific friction be equal to T and the load amplitude of the first cycle be equal to F_1. Increasing load F applied to the model, actuates sliding the spring along the portion $u = F/T$ on each substrate according to Eq. (9) (Fig. 7a). So the whole actuated length of the spring L is equal to $2u$. Portions of this length S retained by friction and R in friction-free state on each substrate are calculated by Eqs. (13) and (14) respectively. Finally Eq. (15) gives the increase in length ΔL of the model as a function of F (Fig. 7a).

Let F_1 denote the magnitudes specifying the load amplitude F_1 (Fig. 7b). After reaching F_1 (Fig. 7b), unloading takes place with F diminishing to zero as shown in Fig. 7c and d. This process is controlled by the same friction gradient T but acting in the direction opposite to a previous one. Now the maximum load $F_{\max}$ in the model is transposed from the gap between the substrates to the friction zones. It travels from the point A (Fig. 7b) to point B (Fig. 7c) pulling part of the spring on the substrates from the gap. The displacement of $F_{\max}$ position into the zone of friction increases the length of the spring involved into frictional contact. It is obvious that at complete unloading ($F = 0$), when $F_{\max}$ decreases to $F_1/2$ (Fig. 7d), a part of the spring AC retained by friction, remains in the stressed state. This causes the appearance of a gap between the substrates representing a residual deformation, ΔL_2.

At the very start of unloading, the length of the spring L_2 is simply equal to R_1, other parts of the spring being intact. However the displacement of $F_{\max}$ inward the substrates increases the length of the actuated spring. Since outside $F_{\max}$ positions (points B in Fig. 7c) the stressed state of the spring remains intact,

which enables one to calculate first the intact length S_0 by Eq. (13) with $F = F_{max}$ and $L = L_1$ and then the sought-for actuated length $L_2 = L_1 - 2S_0$. A portion of L_2, being in frictional contact between the points A and B in Fig. 7c is calculated as

$$S_2 = \int_F^{F_{max}} \frac{df/T}{\sqrt{L_2}(\mathrm{Cth}f - 1/f) + 1}.$$

Now the bridged length of the spring R_2 can be calculated, as $R_2 = L_2 - S_2$, and then its decrease in length ΔL_2 under load F is calculated through Eq. (15).

It is significant that only a portion L_2 of the originally extended spring L_1 participates in the retraction process. Since L_2 is less than L_1 the first is stiffer than the second and causes a steeper unloading curve. The value of R_2 at the end of unloading represents residual deformation.

The second cycle begins with the extension of the system from the state that has resulted after the first cycle (Fig 7d), i.e., with $F = 0$, $L_3 = R_2$, and $R_3 = R_2$. Increasing load sets in motion portions of the spring on the substrates with the load distribution as shown in Fig. 7e for an intermediate state. This process goes on until the load approaches closely the first amplitude value F_1 (Fig. 7f). During this stage of extension, the growing load enlarges the actuated length of the spring L_3 through formation and increase of frictional zone AD as shown in Fig. 7e. Current value of L_3 is calculated by subtracting the intact length of the spring S_3 on the segments DE shown in Fig. 7e the initial total length of the spring equal to $2u_1$. The intact length S_3 in turn consists of two terms: the first is lying between the points E and F and the second between the points F and D

$$s_3 = \int_0^{F_1/2} \frac{df/T}{\sqrt{L_1}(\mathrm{Cth}f - 1/f) + 1} + \int_{F/2}^{F_1/2} \frac{df/T}{\sqrt{L_2}(\mathrm{Cth}f - 1/f) + 1}.$$

So L_3-value is determined as

$$L_3 = 2u_1 - S_3.$$

Now the frictional length S_4 of L_3 can be determined along the segments AD as

$$S_4 = \int_{F/2}^{F} \frac{df/T}{\sqrt{L_3}(\mathrm{Cth}f - 1/f) + 1},$$

and frictionless length R_3 as

$$R_3 = L_3 - S_4.$$

Hence the increase in length is calculated according Eq. (15).

It is important to keep in mind that, since the length of the extending spring L_3 in the second cycle is shorter than that in the first one its elongation at the instant, when the growing load reaches F_1 value, becomes somewhat lower than during the first extension.

However, as soon as the current tensile load F exceeds the previous maximum F_1, the *whole length* of the spring immediately sets in motion according to the Eq. (8) as is shown in Fig. 7f and g. That provokes the stepwise increase in elongation reducing the model to the state characteristic for the one-time extension to the same load F. When the next force amplitude F_2 is reached, the cycle follows the basic pattern of the first cycle. This scheme offers an explanation of restoring the one-time tensile curves during cycling tests with growing load amplitudes.

References

Alexandrov, A.P., Lazurkin, J.S., 1944. Strength of amorphous and crystallizing rubbery Polymer. Dokl. Akad. Nauk USSR. 45, 308–311 (in Russian).

Bokobza, L., 2001. Filled elastomers: a new approach based on measurement of chain orientation. Polymer 42, 5415–5423.

Boonstra, B.B., 1979. Role of particulate filler in elastomer reinforcement: a review. Polymer 20, 691–704.

Boue, F., Vilgis, Th., 1986. Finite extensibility and orientational effects in rubbers. A physical interpretation of the "van der Waals equation" for the elastic force. Colloid Polym. Sci. 264, 285–291.

Dannenberg, E.M., 1966. Molecular slippage mechanism of reinforcement. Trans. Inst. Rub. Ind. 42, 26–42.

Diamant, J., Williams, M.C., Soane, D.S., 1988. Microstructural diagnosis of block copolymers. Nonlinear mechanical properties. 1. Uniaxial stress/strain. Polym. Eng. Sci. 28, 207–220.

Edwards, D.C., 1990. Polymer-filler interactions in rubber reinforcement. J. Mater. Sci. 25, 4175–4185.

Edwards, D.C., Fischer, E., 1973. Wechselwirkung zwischen Polymeren und Fullstof in versterektem Kautschuk. Kaut. Gummi. Kunstst. 26, 46–48.

Eisele, U., Müller, H.-K., 1990. Eine neue Methode zur Bestimmung der Netzstellendichte von gefüllten Vulkanisaten. Kaut. Gummi. Kunst. 43, 9–14.

Grosch, K., Harwood, J.A.C., Payne, A.R., 1966. Breaking energy of rubbers. Nature. N. 5061, 497.

He, T., 1986. An estimate of the strength of polymer. Polymer 27, 253–255.

Heinrich, G., Vilgis, T.A., 1995. Physical adsorption of polymers on disordered filler surfaces. Rub. Chem. Technol. 68, 26–36.

Kaliske, M., Rothert, H., 1998. Int. J. Solids Struct. 35, 2057–2071.

Kilian, H.G., Strauss, M., Hamm, W., 1994. Universal properties in filler-loaded rubbers. Rub. Chem. Technol. 67, 1–16.

Kovrov, V.N., Moshev, V.V., 1984. Mechanical hysteresis in rubbers and its relation to their strength. In: Structure—mechanics studies of composite materials. Urals Branch of the Academy of Sciences of USSR, Sverdlovsk, pp. 19–229 (in Russian).

Kraus, G., 1978. Reinforcement of elastomers by carbon black. Rub. Chem. Technol. 51, 297–321.

Leblanc, J.L., 1995. From peculiar flow properties to reinforcement in carbon black filled rubber compounds. Plast. Rub. Compos. Process. Appl. 24, 241–248.

Medalia, A.I., 1987. Effect of carbon black on ultimate properties of rubber vulcanizates. Rubber chem. technol. 60, 45–61.

Mohsin, M.A., Treloar, L.R.G., 1987. Photoelastic properties of polybutadiene rubbers. J. Polym. Sci. B-Polym. Phys. 25, 2113–2125.

Mullins, L., 1969. Softening of rubber by deformation. Rub. Chem. Technol. 42, 339–362.

Mullins, L., 1987. Engineering with rubber. Chem. Tech. 17, 720–727.

Rigbi, Z., 1980. Reinforcement of rubber by carbon black. Adv. Polym. Sci. 36, 21–68.

Rivin, D., True, R.G., 1973. Filler reinforcement of liquid elastomers. Rubber Chem. Technol. 46, 161–177.

Song, M., 1987. Study on the relationship between the structure of networks and mechanical properties of rubber vulcanizates. 1. The theory of elasticity for rubber vulcanizates with carbon black fillers at large deformations. Polym. Bul. 17, 55–62.

Soos, I., 1984. Charakterisierung des Verstakungeffektes von Fullstoffen aufgrund der Auswertung der Spannungs-Deformations-Kurve. GAK 37, 232–238, 300–303, 509–512.

Treloar, L.R.G., 1958. The Physics of Rubber Elasticity, second ed. Clarendon Press, Oxford.

Voet, A., 1980. Reinforcement of elastomers by fillers: Review of period 1967–1976. J. Polym. Sci. Macromol. Rev. 15, 327–373.

Yuan, Q.W., Kloczkowski, A., Mark, J.E., Sharaf, M.A., 1996. Simulation on the reinforcement of poly(dimethylsiloxane) elastomers by randomly distributed filler particles. J. Polym. Sci. B-Pölym. Phys. 34, 1647–1657.

Yuan, Q.W., Mark, J.E., 1999. Reinforcement of poly(dimethylsiloxane) networks by blended and in-situ generated silica fillers having various sizes, size distributions and modified surfaces. Macromol. Chem. Phys. 200, 206–220.

Zhang, Z.-M., Mark, J.E., 1982. Model networks of end-linked polydimethylsiloxane chains. XIV. Stress-strain, thermoelastic, and birefringence measurements on the bimodal networks at very low temperatures. J. Polym. Sci. Polym. Phys. Ed. 20, 473–480.